



Effect of Sm_2O_3 on structural and thermal properties of zinc fluoroborate glasses

Akshatha WAGH¹, Y. RAVIPRAKASH¹, M. P. AJITHKUMAR², V. UPADHYAYA¹, Sudha D. KAMATH¹

1. Department of Physics, Manipal Institute of Technology, Manipal University, Manipal-576104, Karnataka, India

2. Department of Chemistry, Manipal Institute of Technology, Manipal University, Manipal-576104, Karnataka, India;

Received 19 May 2014; accepted 9 September 2014

Abstract: Glasses based on Sm^{3+} doped zinc fluoroborate were synthesized and characterized. Formations of glasses were investigated in the $30\text{ZnF}_2-20\text{TeO}_2-(50-x)\text{B}_2\text{O}_3-x\text{Sm}_2\text{O}_3$ matrix. Fast quenching and adequate heat treatment are required to prevent melt crystallization and to diminish thermal stress, which result in an efficient amorphous material. The differential scanning calorimetry (DSC), scanning electron microscopy (SEM), energy dispersive X-ray analysis (EDAX), X-ray photoelectron spectroscopy (XPS) were employed to record, calculate, measure and analyze the stability, density and refractive index of the glass samples with different concentrations of Sm^{3+} ranging between 0 to 2.5% (mass fraction). XPS result shows the values of core-level binding energy (Zn 3s, Sm 4d, Te 3d, B 1s, O 1s and F 1s) of ($\text{ZnF}_2\text{-TeO}_2\text{-B}_2\text{O}_3\text{-Sm}_2\text{O}_3$) glass matrix and indicates the good fusibility of the present glass samples. Density of the glass samples increases as dopant concentration increases and glass transition temperature t_g ranges between 395 °C and 420 °C.

Key words: samarium; $\text{ZnF}_2\text{-TeO}_2\text{-B}_2\text{O}_3\text{-Sm}_2\text{O}_3$ glass; rare earth; Hruby's parameter; glass forming ability

1 Introduction

Glasses containing rare earth ions have attracted considerable attention because of their wide applications in laser, up-conversion fluorescence, high density optical storage, solar concentrators, wave-guide lasers fields and other photo-electronic fields [1,2]. The fluoride glasses possess high elasticity and their best attribute is the low optical attenuation. These rare earth doped fluoroborate glasses with various visible emissions will be useful in developing new light sources, display devices, UV sensors and tunable visible lasers [1]. Oxyfluoride glasses are of great interest from the fundamental point of view. The replacement of fluorine by oxygen affects the glass formation and the structure of glass networks, namely, their connectivity. The oxyfluoride glass matrix can provide a unique environment for rare earth ions, which will differ from both the oxide and fluoride matrices. It is expected that oxyfluoride glasses with high content of rare earth elements appear to be new functional materials [1]. Transparent oxyfluoroborate

rare earth doped glasses are interesting class of materials, which combine the optical advantages of fluoride host with the mechanical advantageous of oxide glass plus highest glass formation tendency of borate atoms.

The investigations on absorption properties of the Sm^{3+} ions have indicated that the optical properties of these rare earth ions can be affected by varying the glass composition, thus opening up the possibility of engineering application-friendly compositions [2]. With the increasing demand of various visible lasers and light sources, further investigations in other rare earth ions such as Sm^{3+} ions, are becoming more significant. Oxide glasses are attracting hosts for obtaining efficient luminescence in rare earth ions.

Borate glasses have been widely investigated due to their technological applications. Boron has the highest glass forming tendency because it is in the form of B_2O_3 that does not crystallize by itself even when cooled at the slowest rate [2]. It is a suitable optical material with high transparency, low melting point, high thermal stability and good rare earth solubility. However, interest in borate glass is limited due to its high phonon energy and

it is difficult to obtain high efficient infrared and up-conversion visible emissions. On the other hand, the high phonon energy in borate glass is not detrimental to Sm^{3+} normal 4f transition emissions and sometimes it can accelerate the relaxation processes, which is necessary and beneficial for visible emissions. In this work, borate glass as a suitable host for Sm^{3+} is demonstrated [2].

Lanthanides themselves cannot form glasses, however, they can be incorporated into the structure by associating with the glass composition by introducing as dopants and act as active luminescence centers. It is noted that, when rare earth ions are involved in the matrices, their state determined by the 4f electronic configuration depends weakly on the surrounding ions. The glasses containing oxides and fluorides are appropriate objects for this purpose. Their properties are determined by the relatively low energy of phonons, which is explained by the presence of oxides and the chemical and mechanical stabilities associated with the fluorides [1].

Tellurite glasses are very promising materials for linear and non-linear application in optics, due to some of their important characteristic features such as high refractive index, low phonon maxima and low melting temperature. TeO_2 is known as a conditional glass former, as it needs a modifier in order to form the glassy state easily. Tellurite glasses continue to intrigue both academic and industry researchers not only because of their technical applications, but also owing to a fundamental interest in understanding their microscopic mechanisms. In general, application and utilities of glassy materials are enormous and are governed by the factors like composition, refractive index and dopants present in the glass. Moreover, rare earth in glassy matrix is strongly dependent on crystal field effects, local environment, phonon energies extended into the band gap. It has been found that glasses with a high density along with a low dispersion usually have high non-linear refractive index [3].

B_2O_3 is a glass forming oxide, TeO_2 is a conditional glass former, however, the structural role of zinc in such glasses is the subject of some controversies with evidence for behavior as a network former or a network modifier. Both Zachariasen and Warren's theory of glass structure and Dietzel's crystal field theory classify zinc as a network intermediate, i.e., it is able to adopt both network former and modifier roles depending upon glass matrix [4]. Sm_2O_3 is a modifier in the network. With these chemicals in the glass matrix, a low rate of crystallization, moisture resistant, stable and transparent glasses could be achieved.

The aim of the present work is to describe detailed thermal behavior of oxyfluoroborate glasses, containing

different concentrations of Sm^{3+} and to find correlations between rare-earth content, phase composition and thermal properties of these glasses. To the best of our knowledge, there is a lack of information in the literature about thermal properties of Sm^{3+} -doped oxyfluoroborate glasses. The presented data from the researches indicate that the glass systems with rare earth element that serve as dopants lead to the design of a new material with wide scope in optics and photonics.

2 Experimental

Within the glass forming region of ZnF_2 - TeO_2 - B_2O_3 - Sm_2O_3 glass system, the following compositions with successive increase in the concentration of Sm_2O_3 are chosen for the present work:

Sm_0 : 30ZnF_2 - 20TeO_2 - $50\text{B}_2\text{O}_3$;

Sm_1 : 30ZnF_2 - 20TeO_2 - $49.5\text{B}_2\text{O}_3$ - $0.5\text{Sm}_2\text{O}_3$;

Sm_2 : 30ZnF_2 - 20TeO_2 - $49\text{B}_2\text{O}_3$ - $1.0\text{Sm}_2\text{O}_3$;

Sm_3 : 30ZnF_2 - 20TeO_2 - $48.5\text{B}_2\text{O}_3$ - $1.5\text{Sm}_2\text{O}_3$;

Sm_4 : 30ZnF_2 - 20TeO_2 - $48\text{B}_2\text{O}_3$ - $2.0\text{Sm}_2\text{O}_3$;

Sm_5 : 30ZnF_2 - 20TeO_2 - $47.5\text{B}_2\text{O}_3$ - $2.5\text{Sm}_2\text{O}_3$.

Appropriate amounts of reagent grade ZnF_2 , TeO_2 , B_2O_3 and Sm_2O_3 powders were thoroughly mixed in an agate mortar and the homogeneously mixed materials in porcelain crucibles were heated at $980\text{ }^\circ\text{C}$ in a PID temperature controlled electric furnace (Indfurr Superheat Furnace, with thyristorised control panel (controller/programmer)) for about 1.5 h until a bubble free highly viscous transparent molten mass was formed. The resultant melt was then squeezed on a preheated stainless steel mould and subsequently annealed at $200\text{ }^\circ\text{C}$ for 2 h. The samples were then ground and optically polished using polisher from Chennai Metco Bainpol, Grinding/polishing Machine. The final dimensions of the samples used for structural and thermal analysis were about $0.8\text{ cm}\times 0.8\text{ cm}\times 0.2\text{ cm}$. The density (ρ) of these finely polished glass samples were found through the standard principle of Archimedes in Contech Analytical Balance (with accuracy of 0.0001 g) using xylene (99.99% pure) as the buoyant liquid. The refractive indices of these glasses were measured at lab temperature using Brewster's angle method. The source of monochromatic light was 632.8 nm beam of He-Ne laser. The block diagram of experimental setup is shown in Fig. 1. The polished glass samples were used to reflect the He-Ne laser beam for Brewster's angle measurement. The reflected beam was scanned by means of a laser beam detector. The observations were repeated with different angles of incidence (θ). At the Brewster's angle (θ_B), the difference in the intensity of the two polarized lights reflected from the surface is maximum. Refractive index (n) was calculated using the relation, $n = \tan \theta_B$.

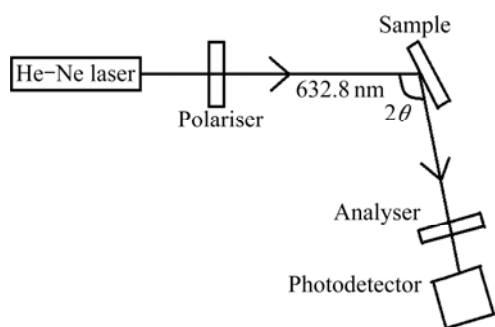


Fig. 1 Schematic diagram of long-arm spectrometer for Brewster's angle measurement

The characteristic temperatures of the glasses were measured using a differential scanning calorimeter (DSC, Shimadzu DSC60) at a heating rate of 10 K/min under controlled atmosphere (N_2). The samples (10–15 mg) were introduced into aluminum pans, which were sealed to prevent the possible contamination of the furnace cell. The estimated values of temperatures were given with an estimated accuracy of ± 2 °C. Chemical analyses were implemented using an energy dispersive X-ray spectrometer (EDAX) and surface morphology was studied through scanning electron microscope (SEM, Zeiss EVO 18 Special).

3 Results and discussion

3.1 Structural analysis

The measurements of density (ρ) and refractive index (n) are the effective tools to explore the degree of structural compactness modification of the geometrical configurations of the glass network [5]. The density and refractive index of the glass samples determined in the present work are given in Table 1 with probable errors of ± 0.001 . The molar volume (V_m) of the glass samples were calculated using the relative molecular mass (M_w) and density (ρ) with the following relation:

$$V_m = M_w / \rho \quad (1)$$

The number density of rare earth [Sm^{3+}] ions (N) was determined using [6]

$$N = (6.023 \times 10^{23} x / \rho) / M_w \quad (2)$$

where x is the mole fraction of cation.

The dielectric constant (ϵ) was calculated using refractive index (n) of the glass,

$$\epsilon = n^2 \quad (3)$$

The molar refractivity (R_m) of the glass samples were calculated using the formula given in Eq. (4) which is well-known as Volf and Lorentz-Lorenz formula [7],

$$R_m = \{[(n^2 - 1)/(n^2 + 2)] \cdot V_m\} \quad (4)$$

where n is the refractive index of the glass sample and V_m is the molar volume (V_m), and $(n^2 - 1)/(n^2 + 2)$ is the reflection loss.

A condition for predicting metallic or insulating behavior in the condensed state matter is metallization criterion, $M = 1 - [R_m/V_m]$. If $R_m/V_m > 1$, the materials show metallic nature and if $R_m/V_m < 1$, they exhibit insulating behavior [8]. The so-called metallization parameter values of the present glasses were found to be less than one and are given in Table 1. Hence, the present glass systems with their metallization parameter values should exhibit insulating nature.

The molar refractivity is related to the structure of the glass and it is proportion to the molar polarizability of the material (α_m) [7]. According to the Clausius-Mosotti relation [7], the molar polarizability of the materials ($10^{-24} \alpha_m \text{cm}^3$) is given by

$$\alpha_m = [(3/4)\pi \times (6.023 \times 10^{23})] \times R_m \quad (5)$$

The electronic polarizability (α_e) can be calculated on the basis of refractive indices using,

$$\alpha_e = [(3(n^2 - 1))/[4\pi \cdot N \cdot (n^2 + 2)]] \quad (6)$$

The obtained values of number density (N) were used to calculate the polaron radius (r_p), inter nuclear distance (r_i) [9,10] and field strength (F) using the following equations respectively:

$$r_p = \frac{1}{2} \left(\frac{\pi}{6N} \right)^{1/3} \quad (7)$$

$$r_i = \left(\frac{1}{N} \right)^{1/3} \quad (8)$$

$$F = Z / (r_p)^2 \quad (9)$$

where Z is the atomic number of Sm^{3+} ion.

The variation of molar volume, density, electronic polarizability, number density of glasses with different compositions of Sm_2O_3 is shown in Figs. 2(a) and 2(b) respectively. Figure 3 indicates the variation of polaron radius (r_p) and field strength (F) with different concentrations of Sm_2O_3 .

It is evident from Figs. 2(a) and 2(b) and also Table 1 that the density, molar volume, number density of the samarium ions of the present glass system increases with increase in the content of Sm_2O_3 . The dielectric constant is directly correlated with the polarizability of the glass. The dielectric constant gradually increases with the increase in the Sm_2O_3 content in the glasses. Hence, the electronic polarizability decreases with the increase in dielectric constants which is clearly evident through Table 1.

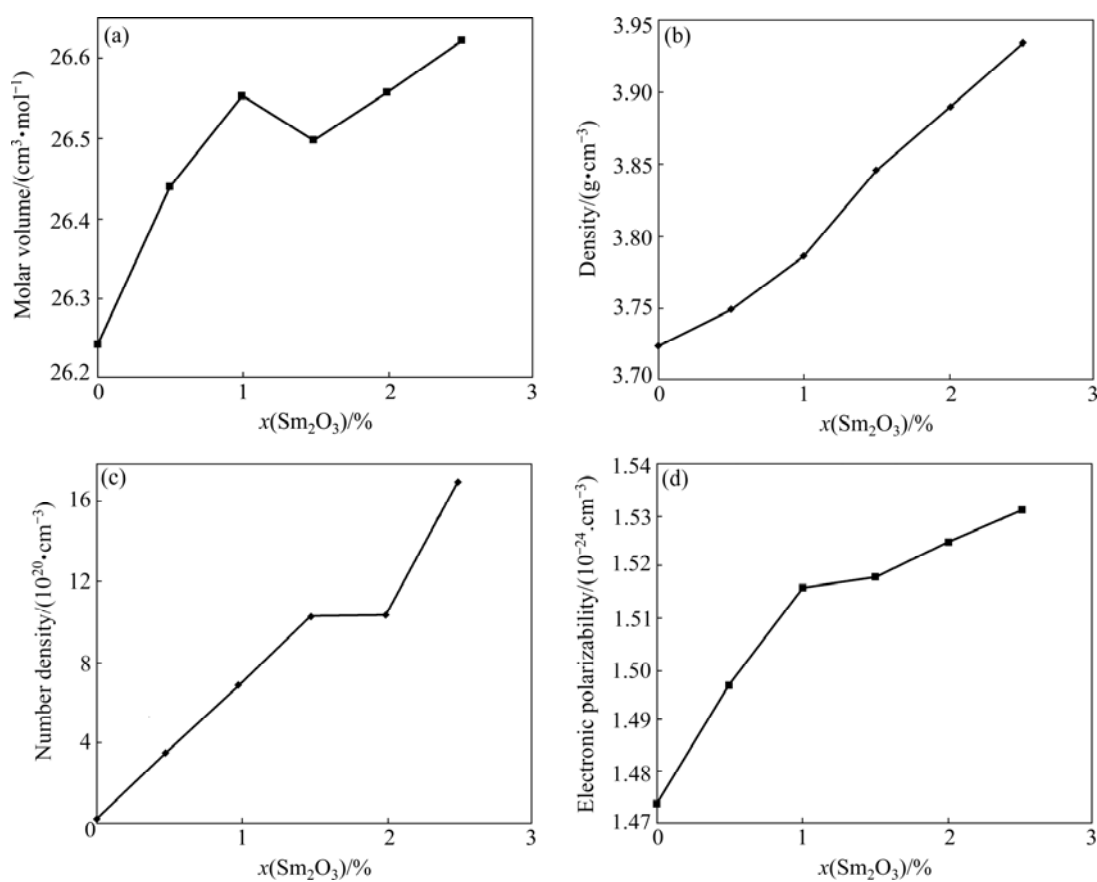


Fig. 2 Variation of molar volume (a), density (b), number density (c) and electronic polarizability (d) of glasses with different compositions of Sm₂O₃

Table 1 Physical parameters of 30ZnF₂–20TeO₂–(50–x)B₂O₃–xSm₂O₃ glass system

Parameter	Sm ₀	Sm ₁	Sm ₂	Sm ₃	Sm ₄	Sm ₅
Average relative molecular mass/(g·mol ⁻¹)	97.7000	99.1000	100.5000	101.9000	103.3000	104.7000
Density, ρ /(g·cm ⁻³)	3.7240	3.7494	3.7860	3.8466	3.8903	3.9328
Refractive index, n	1.4510	1.4575	1.4610	1.4615	1.4620	1.4630
Optical dielectric constant, ϵ	2.1054	2.1243	2.1345	2.1359	2.1374	2.1403
Molar volume, V_m /(cm ³ ·mol ⁻¹)	26.2300	26.3300	26.4300	26.4900	26.5500	26.6200
Molar refractivity, R_m /(cm ³ ·mol ⁻¹)	7.0600	7.1700	7.2600	7.2700	7.3000	7.3300
$1-(R_m/V_m)$	0.730	0.7270	0.7250	0.7250	0.7250	0.7240
Number density, N /(10 ²⁰ ·cm ⁻³)	–	3.4300	6.8300	10.2300	10.3600	16.9700
Inter ionic distance, $r_i/\text{Å}$	–	14.2900	11.3400	9.9200	9.8800	8.3800
Polaron radius, $r_p/\text{Å}$	–	5.7500	4.5700	4.0000	3.9800	3.3700
Field strength, F /(10 ¹⁵ ·cm ⁻²)	–	3.0400	4.8200	6.3000	6.3500	8.8200
Electronic polarizability, $\alpha_0^{2-}(n)$ /(10 ⁻²⁴ ·cm ³)	1.474	1.4970	1.5160	1.5180	1.5250	1.5310
Molar electronic polarizability α_m /(10 ⁻²⁴ ·cm ³)	2.798	2.848	2.8780	2.8820	2.8930	2.9050

The observed decrease of polaron radius (r_p) with increasing Sm₂O₃ content is most likely related to the increased value of number density (N) for Sm³⁺ ions. The Sm³⁺ ions are situated between the layers and thus the distance between Sm³⁺ ions and oxygen atoms decrease.

As a result, the Sm—O bond strength increases, producing a stronger field around the Sm³⁺ ions.

The chemical compositions of the constituent elements for the thermally evaporated glass sample (where $x=2.5\%$) have been investigated by means of an

energy dispersive X-ray analysis (EDAX) unit interfaced with scanning electron microscope (SEM). The SEM image of the 2.5% Sm_2O_3 doped glass shown in Fig. 4(a) indicates the amorphous nature of the sample. In SEM micrograph, the nearly perfect homogeneity is observed and unsolved particles were not seen. Doping Sm_2O_3 into zinc fluoroborate glass gives fine surface feature. Figure 4(b) show the EDAX spectrum of 2.5% Sm_2O_3 doped glass. The obtained data showed all the glass chemicals like samarium (Sm), tellurium (Te), zinc (Zn), oxygen (O), boron (B) and fluorine (F), thus proving the

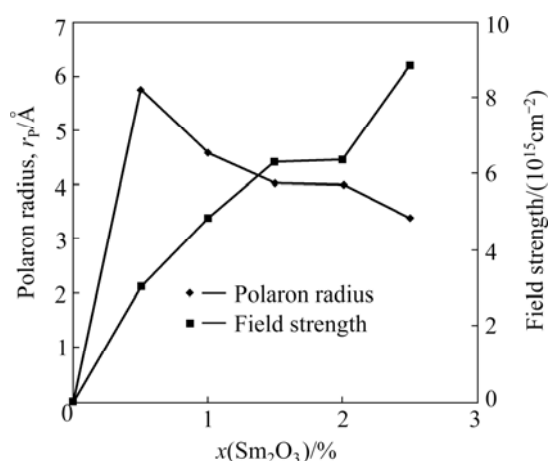


Fig. 3 Variation of polaron radius and field strength of glass with different contents of Sm_2O_3

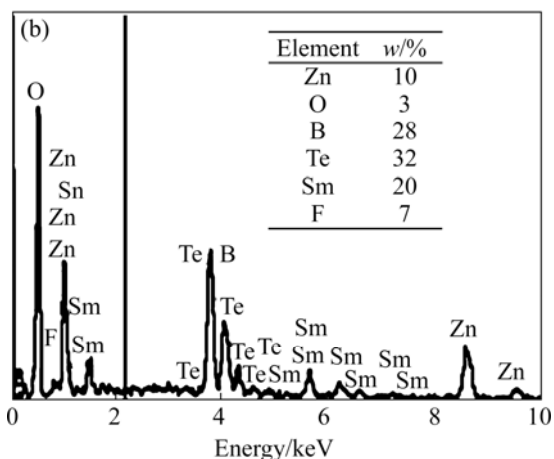
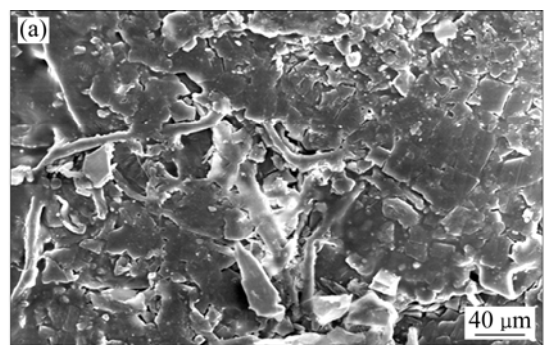


Fig. 4 SEM image (a) and EDAX spectrum (b) of 2.5% Sm_2O_3 doped glass matrix

existence of all the major elements used in the building the sample.

3.2 X-ray photoelectron spectroscopy (XPS)

The composition and the fusibility of different chemicals added in the preparation of the glass samples were studied by X-ray photoelectron spectroscopy, performed in a ESCA microprobe with a monochromatic X-ray source of Al K_{α} radiation. The pressure in the analysis chamber was lower than 10^{-8} Pa and the source characteristics were of 10 kV and 5 mA. A freshly abraded silver paste was used for standardizing the BEs of the spectrometer on the well-known Ag $3d_{3/2}$ and Ag $3d_{5/2}$ XPS transitions at 374.3 and 368.3 eV, respectively. As charging effects are unavoidable in the XPS [11,12] study of our insulating glass samples, the BE was calibrated with contamination carbon in each sample. For this internal reference, we used the C 1s level of unsaturated hydrocarbons at 284.6 eV. A plot of measured BE values of Zn 3s, Sm 4d, Te 3d, B 1s, O 1s and F 1s of 2.5% Sm_2O_3 doped glass sample by XPS with charging corrections is shown in Fig. 5.

The measured BE values of the elements present in the $\text{ZnF}_2\text{-TeO}_2\text{-B}_2\text{O}_3\text{-Sm}_2\text{O}_3$ glass matrix for 2.5% Sm_2O_3 doped glass are given in Table 2. The similar peaks were also observed in other samples with slightly variations in peak intensity. In the present XPS work on ($\text{ZnF}_2\text{-TeO}_2\text{-B}_2\text{O}_3\text{-Sm}_2\text{O}_3$) glass sample, slightly greater BE values were observed for all compounds (Sm, Zn, Te, B, O, F) as compared their BEs with literature referenced values. It may be attributed to water adsorbed (OH adsorbed) during the formation of the pellet [11–13].

Table 2 Binding energy (BE) values of element's photoelectron peak in 2.5% Sm_2O_3 doped sample (BE values are corrected from contamination carbon at 284.6 eV)

Element	BE/eV
Oxygen (O 1s)	538.2
Boron (B 1s)	196.8
Zinc (Zn 3s)	144.2
Fluorine (F 1s)	687.3
Tellurium (Te 3d)	581.9, 592.4
Samarium (Sm 4d)	135.6

3.3 Thermal analysis

No simple way currently exists to formulate the correlation between the ideal composition and the stability of these types of glasses. Different simple quantitative methods have been suggested in order to evaluate the level of stability of the glass alloys. Most of them are based on the characteristic temperatures such as the glass transition temperature (t_g), the temperature at

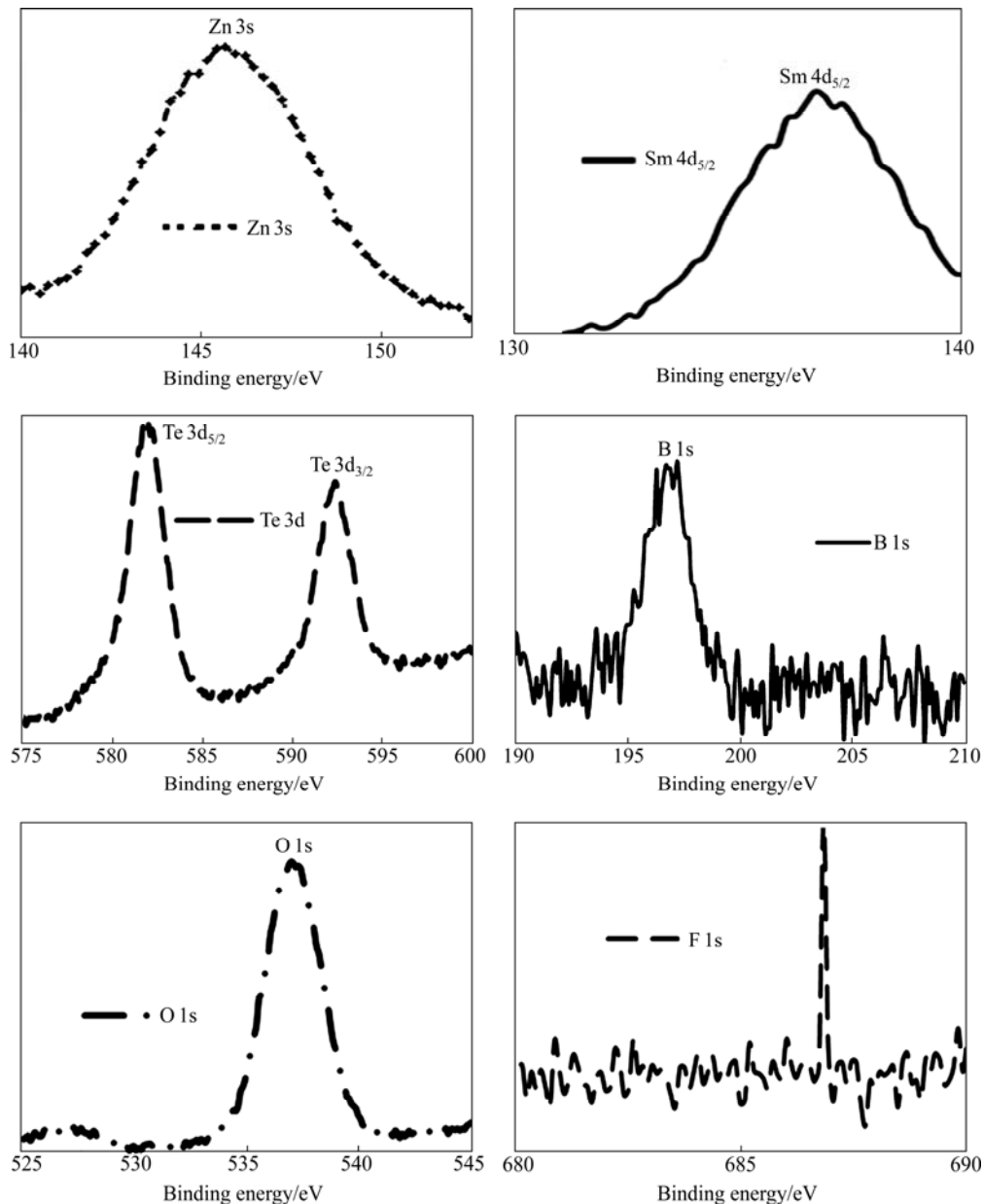


Fig. 5 XPS BE spectra of Zn 3s, Sm 4d, Te 3d, B 1s, O 1s and F 1s energy levels of 2.5% Sm₂O₃ doped glass sample

which crystallization begins (t_c), the temperature corresponding to the maximum crystallization rate (t_p), or the melting temperature (t_m). Some of the suggested methods are based on the crystallization activation energy. The characteristic temperatures (t_g , t_c , t_p and t_m) are easily and accurately obtained by the differential scanning calorimetry (DSC) during the heating process of the glass sample. Dietzel introduced the first glass criterion, $\Delta t = t_c - t_g$, which is often an important parameter to evaluate the glass forming ability of the glasses [14,15]. In the present work, the results are focused over 2.5% Sm₂O₃ doped glass sample which showed good results compared to other samples. The above mentioned criteria have been applied to the 2.5% Sm₂O₃ doped glass in temperature range of 100–600 °C. Mass loss values

were observed through TGA in the temperature range between 350–580 °C which are clearly indicated in the DSC plot under the same temperature range which may be due to evaporation of some fluorine (F) content (Fig. 6(a)). The DSC curve includes temperature of glass transition (t_g), the onset of crystallization (t_c) and the exothermic maximum (t_p) (Fig. 6(b)). In most cases, the melting temperature (t_m) does not appear in DSC traces, as it is higher than 600 °C. An appropriate value may be found by applying the classical two-thirds rule expressed as $t_g/t_m = 2/3$ [16].

The curve exhibits an endothermic effect due to glass transition temperature t_g . The value of t_g is evaluated from the point of inflection of this change. At still higher temperature, an exothermic peak t_c due to

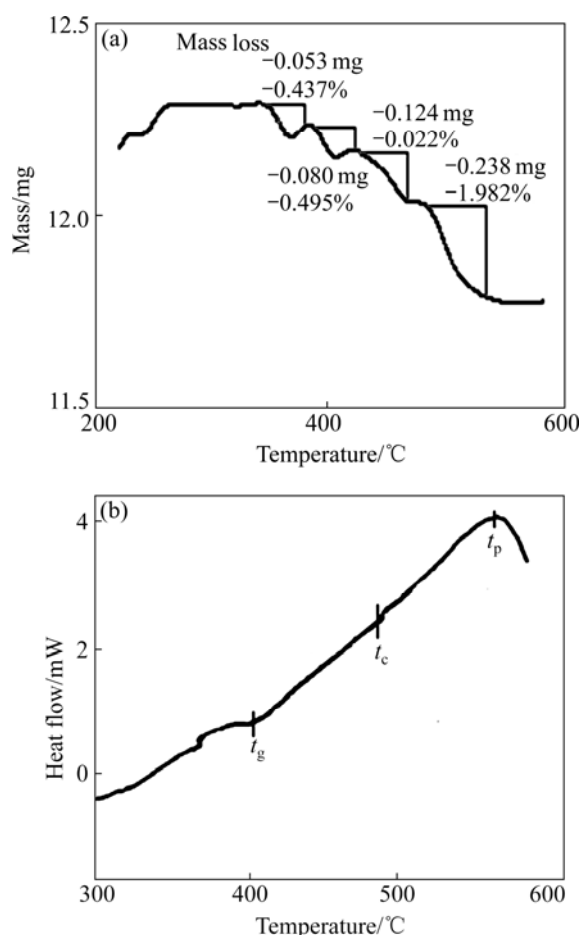


Fig. 6 TG analysis (a) and DSC thermogram (b) of 2.5% Sm₂O₃ doped sample

crystal growth followed by an endothermic effect due to the melting effect denoted by t_m was also studied through classical two-thirds rule [14].

Glass stability may be evaluated using semi-empirical relations based on characteristic temperatures. The thermal stability range ($t_c - t_g$) provides a good estimate of the tendency of the glass to crystallization state. It should usually be larger than 100 °C to obtain a stable sample [14–17]. A popular stability scale is based on the Hruby's criterion [14,15] defined as $H_r = [(t_c - t_g) / (t_m - t_c)]$. This parameter, which depends on t_c , t_g

and t_m of a glass, gives information about glass forming ability (GFA) and glass thermal stability (GTS). A wider gap in the ($t_c - t_g$) gap results from a drop in the glass viscosity [18], while the denominator ($t_m - t_c$) is influenced by the magnitude of the growth rate. If the gap ($t_m - t_c$) decreases, the crystal growth rate falls rapidly and GFA increases. The larger difference $\Delta t = t_c - t_g$ and the smaller temperature interval $t_m - t_c$ hamper the processes of crystallization, and consequently facilitate glass formation. The parameters GFA and GTS are directly proportional to ($t_c - t_g$) and inversely proportional to ($t_m - t_c$).

The introduction of rare earth oxides decreases the viscosity and melting temperature of rare earth doped glasses [18]. In the present work, the increase in rare earth oxide (Sm₂O₃) content with replacement of B₂O₃ must have decreased the glass viscosity and the magnitude of the growth rate by increasing the crystalline temperature (t_c) and decreasing the melting temperature (t_m).

Another stability scale introduced by KLOUCHE BOUCHAROUR [16] takes into account the difference between t_p and t_c , which depends on the width of the crystallization peak. When the ($t_p - t_c$) factor is high, the growth rate decreases. This criterion is defined as follows: $S = [(t_p - t_c) \cdot (t_c - t_g)] / t_g$ [14]. When the ($t_p - t_c$) factor is high, the growth rate decreases and GFA increases.

The variations of t_g , t_c , t_p , t_m , H_r , S with the Sm₂O₃ content in 30ZnF₂-20TeO₂-(50-x)B₂O₃-xSm₂O₃ ($x=0, 0.5, 1.0, 1.5, 2.0, 2.5$) are shown in Figs. 7(a) and 7(b) and the tabulated values of these parameters are given in Table 3.

For 2.5% doped Sm₂O₃ glass, H_r (0.732) and S (21.8) values were found to be maximum as compared with other doped glasses investigated in this work. This proves the good glass forming ability (GFA) and glass thermal stability (GTS) of 2.5% Sm₂O₃ doped glass.

All the quantities of the glass samples (Δt , H_g , H_r and S) follow the same trend which indicates the good homogeneity of the glasses prepared. The thermal stability of a glass depends on Δt that increases with the increase in Sm₂O₃ content. In other words, the addition of samarium enhances the glass formation ability.

Table 3 Thermal stability parameters of zinc fluoroborate glasses for samarium series at a heating rate of 10 K/min

Sample	$x(\text{Sm})/\%$	$t_g/^\circ\text{C}$	$t_c/^\circ\text{C}$	$t_p/^\circ\text{C}$	$t_m/^\circ\text{C}$	$\Delta t = t_c - t_g$	$\Delta t = t_m - t_c$	H_g	H_r	S
Sm ₀	0	420	480	568	630	60	150	0.142	0.4	12.6
Sm ₁	0.5	410	495	560	615	85	120	0.207	0.708	13.5
Sm ₂	1.0	408	480	555	612	72	132	0.176	0.545	13.2
Sm ₃	1.5	405	480	548	608	75	128	0.185	0.585	12.6
Sm ₄	2.0	395	464	545	593	69	129	0.174	0.534	14.1
Sm ₅	2.5	401	486	589	602	85	116	0.211	0.732	21.8

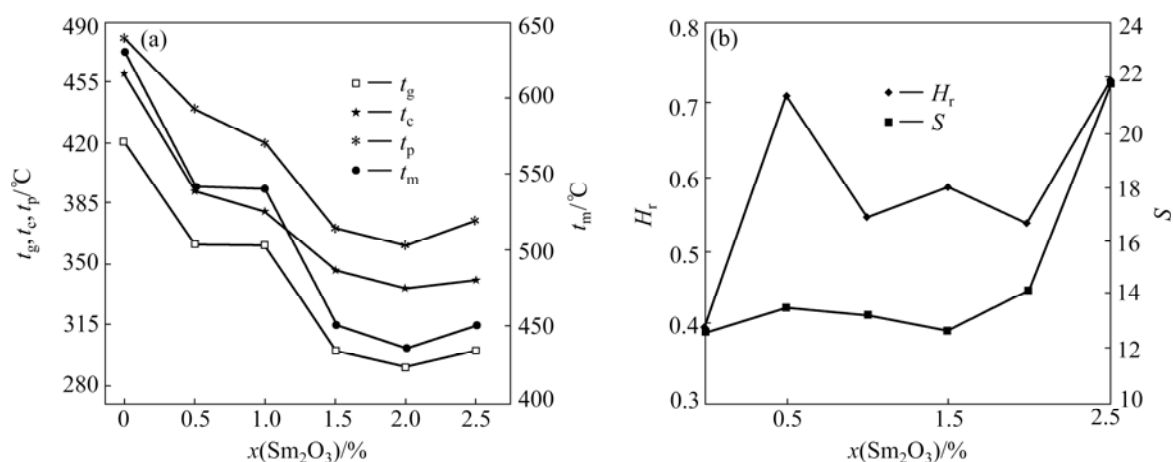


Fig. 7 Evolution of characteristic temperatures (t_g , t_c , t_p , t_m) (a) and stability criteria versus Sm₂O₃ content (b) in 30ZnF₂-20TeO₂-(50-x)B₂O₃-xSm₂O₃ ($x=0, 0.5, 1.0, 1.5, 2.0, 2.5$) glasses

4 Conclusions

1) The structural and thermal properties for the ZnF₂-TeO₂-B₂O₃-Sm₂O₃ glasses were evaluated by using various criteria. The H_r criteria were considered for the evaluation of glass stability by using DSC thermogram. The obtained results of Δt , H_g , H_r and S criteria agree satisfactorily with the DSC and TGA data. The Sm₅ glass sample showed the good stability factor.

2) These nonmetallic Sm³⁺ doped glasses exhibited fine structural compactness with high density values and also through other calculated physical parameters like molar volume, number density, electronic polarizability etc.

3) SEM/EDAX and XPS revealed the good homogeneity and fusibility of the glass samples. These findings revealed that the Sm₅ glass sample has maximum stability to atmospheric moisture.

4) In all, the present Sm³⁺ doped glasses can be used in working models of optoelectronics and photonics.

References

- [1] POLISHCHUK S A, IGNAT' EVA L N, MARCHENKO Y V, BOUZNIK V M. Oxyfluoride glasses (A review) [J]. Glass Physics Chemistry, 2011, 37(1): 1–20.
- [2] LIN H, YANG D, LIU G, TIECHENG M, ZHAI B, QINGDA A, YU J, WANG X, LIU X, BUN PUN E Y. Optical absorption and photoluminescence in Sm³⁺- and Eu³⁺-doped rare-earth borate glasses [J]. Journal of Luminescence, 2005, 113: 121–128.
- [3] ERAIAH B. Optical properties of lead-tellurite glasses doped with samarium trioxide [J]. Bulletin of Material Science, 2010, 33(4): 391–394.
- [4] CASSINGHAM N J, STENNETT M C, BINGHAM P A, AQUILANTI G, HYATT N C. The role of Zn in model nuclear waste glasses studied by XAS [C]// Diamond'10 Conference Decommissioning, Immobilisation and Management of Nuclear Waste for Disposal. Manchester, UK, 2010.
- [5] ERAIAH B. Optical properties of samarium doped zinc-tellurite glasses [J]. Bulletin of Material Science, 2006, 29(4): 375–378.
- [6] CHIMALAWONG P, KIRDSIRI K, KAEWKHAO J, LIMSUWAN P. Investigation on the physical and optical properties of Dy³⁺ doped soda-lime-silicate glasses [J]. Procedia Engineering, 2012, 32: 690–698.
- [7] KAEWWISET W, KAEWKHAO J, LIMSUWAN P. UV-visible-NIR study of Er³⁺ doped soda lime silicate glass [J]. Asian Journal on Energy and Environment, 2010, 11(1): 37–47.
- [8] LAKSHIMI SRINIVASA RAO S, RAMDEVUDU G, SHAREFUDDIN Md, ABDUL HAMEED, NARASIMHA CHARY M, LAKSHMIPATHI RAO M. Optical properties of alkaline borate glasses [J]. International Journal of Engineering Science, and Technology, 2012, 4(4): 25–35.
- [9] SAYED MOUSTAFA EI, SADDEEK Y B, SHAABAN E R. Structural and optical properties of lithium borobismuthate glasses [J]. Journal of Physics and Chemistry of Solids, 2008, 69: 2281–2287.
- [10] RAGHAVENDRA RAO T, RAMA KRISHNA C, UDAYACHANDRAN THAMPY U S, VENKATA REDDY C, REDDY Y P, SAMBASIVA RAO P, RAVIKUMAR R V S S N. Effect of Li₂O content on physical and structural properties of vanadyl doped alkali zinc borate glasses [J]. Physica B, 2011, 406: 2132–2137.
- [11] LI Dong-sheng, ZHANG Xu-wu, LU Jin, YANG De-ren. Structure and luminescence evolution of annealed europium-doped silicon oxides films [J]. Optics Express, 2010, 18(26): 27191–27196.
- [12] MERCIER F, ALLIOT C, BION L, THROMAT N, TOULHOAT P. XPS study of Eu(III) coordination compounds: Core levels binding energies in solid mixed-oxo-compounds Eu_mX_nO_y [J]. Journal of Electron Spectroscopy and Related Phenomena, 2006, 150/1: 21–26.
- [13] JI Guo-jun, SUI Zhi-ming. AFM and XPS study of glass surface coated with titania nanofilms by sol-gel [J]. Chinese Physics Letters, 2010, 27(9): 096801–096804.
- [14] SAILAJA G, NAGALAKSHMI T V, VEERABHADRA RAO A, EMMANUEL K A. Structural study of PbO-NaF-B₂O₃ glass system doped with Cr₂O₃ through spectroscopic and magnetic properties international journal of chemical [J]. Environmental and Pharmaceutical Research, 2011, 2(2–3): 101–110.
- [15] ALY K A, DAHSHAN A, ABDEL-RAHIM F M. Thermal stability of Ge-As-Te-In glasses [J]. Journal of Alloys and Compounds,

2009, 470: 574–579.

- [16] KLOUCHE BOUCHAOUR Z C, POULAIN M, BELHADJI M, HAGER I, MALLAWANY R El. New oxyfluoroniobate glasses [J]. Journal of Non crystalline Solids, 2009, 351: 818–825.
- [17] PABLICK C. Europium doped fluorozirconate-based glasses or

medical and photovoltaic applications [D]. Paderborn University of Paderborn, 2009.

- [18] WANG Mi-tang, CHENG Jin-shu, MEI L I. Effect of rare earths on viscosity and thermal expansion of soda–lime–silicate glass [J]. Journal of Rare Earths, 2010, 28: 308–311.

Sm₂O₃ 对含 Zn 氟硼酸盐玻璃结构和热性能的影响

Akshatha WAGH¹, Y. RAVIPRAKASH¹, M. P. AJITHKUMAR², V. UPADHYAYA¹, Sudha D. KAMATH¹

1. Department of Physics, Manipal Institute of Technology, Manipal University, Manipal-576104, Karnataka, India

2. Department of Chemistry, Manipal Institute of Technology, Manipal University, Manipal-576104, Karnataka, India;

摘要: 合成 Sm³⁺ 掺杂含锌氟硼酸盐玻璃并对其表征。研究 30ZnF₂-20TeO₂-(50-x)B₂O₃-xSm₂O₃ 的玻璃形成能力。为防止熔体结晶和消除热应力，以得到非晶材料，必须对材料进行快速淬火和适当的热处理。采用 DSC、SEM、EDAX、XPS 研究含不同 Sm³⁺ 浓度(0–2.5%，质量分数)玻璃样品的稳定性、密度和折射率。采用 XPS 对 ZnF₂-TeO₂-B₂O₃-Sm₂O₃ 基玻璃的内层电子结合能(Zn 3s, Sm 4d, Te 3d, B 1s, O 1s 和 F 1s)进行分析，结果表明该玻璃样品具有良好的可溶性。玻璃样品的密度随掺杂剂浓度的增加而增加，玻璃转变温度 t_g 在 395~420 °C 之间变化。

关键词: 钐; ZnF₂-TeO₂-B₂O₃-Sm₂O₃ 玻璃; 稀土; Hruby 参数; 玻璃形成能力

(Edited by Yun-bin HE)